Effect of the Bandgap, Sun Concentration and Surface Recombination Velocity on the Performance of a III-V Bismide Multijunction Solar Cells

Abu Kowsar*, Syed Farid Uddin Farhad*‡ and Syed Nazmus Sakib**

*Solar Energy Conversion and Storage Research Section, Industrial Physics Division, BCSIR Laboratories, Dhaka, Bangladesh Council of Scientific and Industrial Research (BCSIR), Dhaka-1205, Bangladesh.

**Department of Electronics and Telecommunication Engineering, Daffodil International University, Dhaka-1207, Bangladesh

(apukowsar@gmail.com, sf1878@my.bristol.ac.uk, nazmus.ete@diu.edu.bd)

‡ Corresponding Author: Syed Farid Uddin Farhad, Industrial Physics Division, BCSIR Laboratories, Dhaka, Bangladesh Council of Scientific and Industrial Research (BCSIR), Dhanmondi, Dhaka-1205, Tel: +88 01881755767,

Received: 11.10.2018 Accepted:22.11.2018

Abstract- In this paper, an emerging material $GaAs_{1-x}Bi_x$ has been introduced in different layers of multijunction solar cells. By modifying the spectral p-n junction model, the theoretical efficiencies of two-, three- and four-junction III-V bismide multijunction solar cells have been estimated to be 36.5%, 44.0%, and 52.2% respectively for AM1.5G under 1 sun condition. The effects of the material bandgap, sun concentration, and surface recombination velocity on the cell performance have been studied extensively. Simulation results revealed that an increment up to ~10% on the overall cell efficiency can be achieved by concentrating the solar radiation from 1 sun to 500 sun; and a 3 – 4 % increment on the overall cell efficiency by tuning the bandgap of the bismide layer as well as modeling the surface recombination velocity involved. These simulation results could be utilized for better understanding the materials as well as in realization of highly efficient bismide based multijunction solar cells.

Keywords III-V bismide; multijunction solar cell; bandgap tuning; surface recombination velocity.

1. Introduction

Multijunction solar cells are judiciously designed in order to capture light from near UV to mid-IR region of the solar spectrum. To achieve very high efficiency, different research groups reported different types of multijunction solar cells in different new approaches. In this direction, Gallium indium phosphide ($GaInP_2$) and Gallium arsenide (GaAs) have been extensively used as top and middle layer [1] and Germanium (Ge) as bottom layer [1, 2] in different multijunction solar cells. Indium gallium arsenide (InGaAs) has also been used as the bottom layer instead of Ge layer [3]. Recently, another emerging III-V semiconductor alloy Gallium Arsenic Bismide ($GaAs_{1-x}Bi_x$) has attracted much attention due to its' suitable optoelectronic parameters such as bandgap, electron and hole mobility, doping concentrations etc. to realize high-efficiency multijunction solar cell [4-9]. The bandgap of GaAs was reported to be reduced by ~ 84 meV for each 1% percent of bismuth (Bi) content (x) [10-13]. Since a very small amount of Bi is incorporated in the GaAs matrix, therefore, the lattice constant of the synthesized material is assumed to be almost the same [12, 13]. $GaAs_{1-x}Bi_x$ can offer tunable bandgap when Bi is incorporated with GaAs rather than that of the fixed bandgap of Ge of standard multijunction cells [2]. This is similar to InGaAs compound which provides tunable bandgap when indium (In) is incorporated with GaAs [14]. More importantly, all these semiconductors possess direct bandgap (Eg) with zinc blende crystal structure as well as they are lattice-matched materials for different cell combinations [15].

In this work, $GaInP_2$ was used as a top layer in all cell combinations; GaAs as a second layer for three-junction (3J) and four-junction (4J) solar cell, an emerging material $GaAs_{1-x}Bi_x$ was used as a bottom layer (also third layer for the 4J cell) for all combination as diagramed in Fig.1. This material could be obtained by mixing of appropriate mole fraction of Bi

content with GaAs (Eg = 1.42eV). To the best of our knowledge, this kind of performance analysis for bismide based multijunction solar cells has not been explored previously. Therefore, in this work we consider a number of crucial solar cell parameters and their impact project to enhance our understanding about bismide based solar energy materials as well as to investigate its potentials for integrating it into the multijunction solar cells. The main focus of this work is to analyze the impact of different factors on the efficiencies of these III-V bismide multijunction solar cells. In this paper, the short-circuit current density (Jsc), the reverse saturation current density (Jo), the open circuit voltage (Voc), the voltage (Vm) at maximum power point, and the current density (Jm) at maximum power point, fill-factor (FF) and efficiencies (η) have been studied. Finally, the performance of the novel III-V bismide multijunction cells with varying bandgap of bismide materials, sun concentration, and surface recombination velocities have been studied extensively. Different optoelectronic characteristics and the efficiency of our proposed multijunction solar cell are estimated by invoking modified version of standard solar cell equations [11-15]. This is basically a modification of the spectral p-n junction model proposed by Nell and Barnett [13].

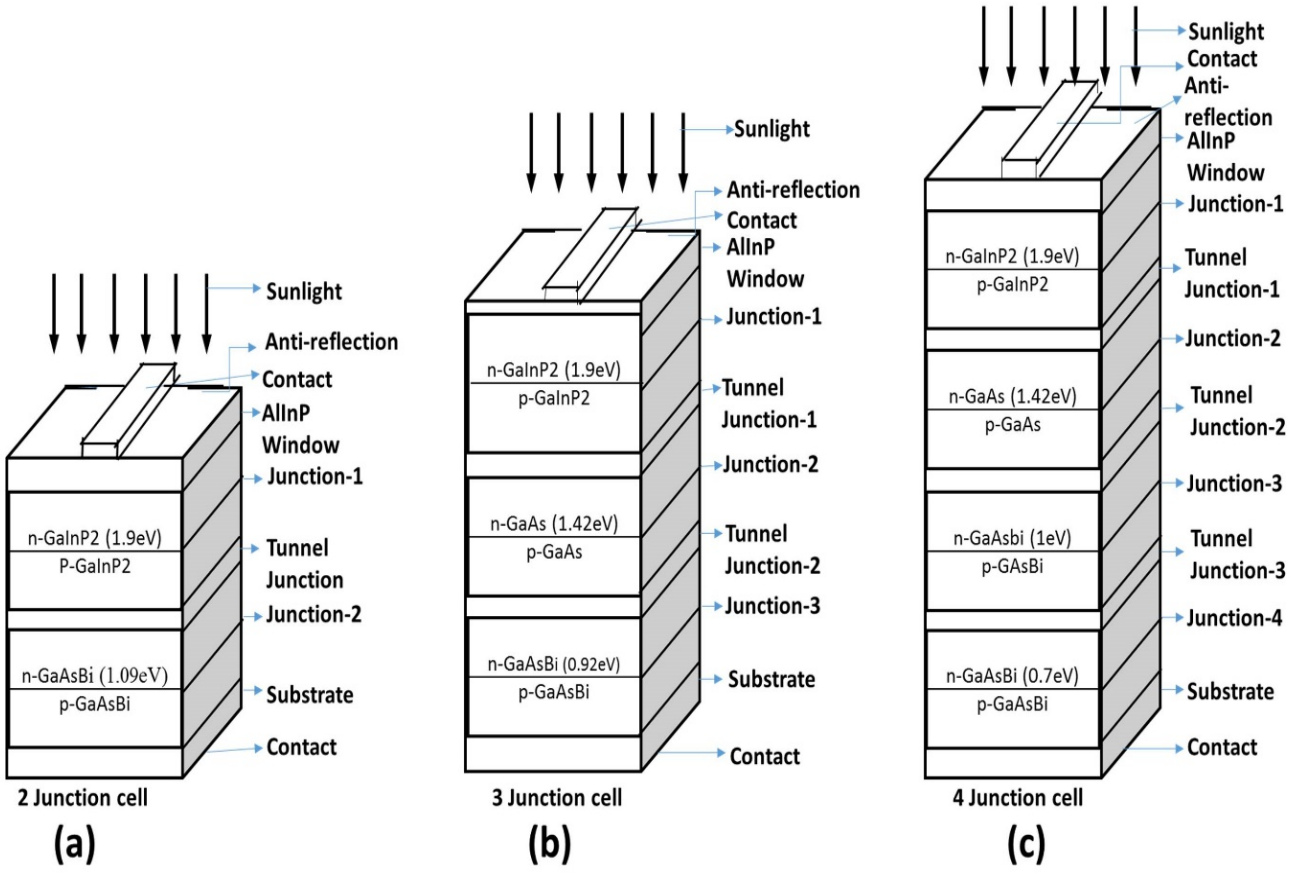

Fig. 1. Schematic diagrams of 2-Junction (a), 3-Junction (b), and 4-Juntion (c) III-V Bismide multijunction solar cells (different cell components are not drawn to scale).

2. Theoretical Model

In the multijunction solar cell, solar spectrum is usually split into parts and each part of the spectrum is absorbed in the suitable bandgap sub-cells. The sub-cells are stacked in order of higher bandgap to lower bandgap and they are connected in series. Note that we assume zero series resistance and infinite shunt resistance in our model. However, the electrical characteristics of these multijunction solar cells have been determined using a modified version of the standard equations [9, 13, 15-23]. According to this model, the short-circuit current density (J_{sc}), has been determined directly from the

reference spectra [24, 25] of American Society for Testing and Materials (ASTM):

$$J_{sc} = e \times \frac{\square I}{h\nu} \quad (1)$$

Here, e is the charge of an electron, I is the irradiance and λ is the wavelength of incident light, h is the Plank's constant and v is the velocity of light

The reverse saturation current density (J_0) is a very important factor for cell performance that is determined for each cell as the sum of the currents for the n-type and p-type layers [17].

$$J_0 = e\left(\frac{D_e}{\tau_e}\right)^{\frac{1}{2}}\frac{n_i^2}{N_A}\left(\frac{S_e(\frac{\tau_e}{D_e})^{\frac{1}{2}}\cosh\left(\frac{x_p}{\sqrt{D_e\tau_e}}\right)+\sinh\left(\frac{x_p}{\sqrt{D_e\tau_e}}\right)}{S_e(\frac{\tau_e}{D_e})^{\frac{1}{2}}\sinh\left(\frac{x_p}{\sqrt{D_e\tau_e}}\right)+\cosh\left(\frac{x_p}{\sqrt{D_e\tau_e}}\right)}\right) + \left(\frac{D_h}{\tau_h}\right)^{\frac{1}{2}}\frac{n_i^2}{N_D}\left(\frac{S_h(\frac{\tau_h}{D_h})^{\frac{1}{2}}\cosh\left(\frac{x_n}{\sqrt{D_h\tau_h}}\right)+\sinh\left(\frac{x_n}{\sqrt{D_h\tau_h}}\right)}{S_h(\frac{\tau_h}{D_h})^{\frac{1}{2}}\sinh\left(\frac{x_n}{\sqrt{D_h\tau_h}}\right)+\cosh\left(\frac{x_n}{\sqrt{D_h\tau_h}}\right)}\right) \quad (2)$$

Here, D_e and D_h stand for diffusion constant for electron and hole, τ_e and τ_h are the minority carrier lifetime for electron and hole, n_i is the intrinsic carrier concentration, N_A and N_D are the acceptor and the donor concentration, S_e and S_h are the surface recombination velocity of electron and hole, X_h and X_p are the thickness of p-layer and n-layer respectively.

The diffusion constants D_e and D_h are calculated from the Einstein's relationship:

$$D_e = \frac{kT\mu_e}{e} \quad (3)$$

$$D_h = \frac{kT\mu_h}{e} \quad (4)$$

Here, μ_e and μ_h are the mobility of electron and hole respectively and k is the Boltzmann constant.

The minority carrier lifetime τ_e and τ_h are calculated from

$$\frac{1}{\tau_e} = \frac{1}{\tau_{SRH}} + BN_A \quad (5)$$

$$\frac{1}{\tau_h} = \frac{1}{\tau_{SRH}} + BN_D \quad (6)$$

Here, τ_{SRH} is the Shockley-Read-Hall lifetime and B is the direct band-band recombination coefficient.

The surface recombination velocities of electron S_e and hole S_h are determined from

$$S_e = \frac{D_e}{L_e} = \frac{D_e}{\sqrt{\tau_e D_e}} = \sqrt{\frac{D_e}{\tau_e}} \quad (7)$$

$$S_h = \frac{D_h}{L_h} = \frac{D_h}{\sqrt{\tau_h D_h}} = \sqrt{\frac{D_h}{\tau_h}} \quad (8)$$

The intrinsic carrier concentration n_i is determined from

$$n_i^2 = 4M_cM_v\left(\frac{2\pi kT}{h^2}\right)^3(m_e^*m_h^*)^{\frac{3}{2}}exp\left(\frac{-E_g}{kT}\right) \quad (9)$$

Here, E_g is the bandgap energy of the semiconductor, T is the temperature, M_c and M_v denote the number of equivalent minima in the conduction band and valance band, m_e^* and m_h^* are the effective mass of electrons and holes respectively. Photons with energy higher than the material bandgap (E_g) generate power to the cell output and release excessive energy as heat into the cell, while photons with lower energy than E_g are transmitted to lower sub-cell.

The total current density (J) is

$$J = J_0\left(e^{\frac{qv}{KT}} - 1\right) - J_{ph} \quad (10)$$

Here, J_{ph} is the light generated current density, Jo is the reverse saturation current density, q is the elementary charge, K is the Boltzmann constant and T is the temperature.

The maximum power density condition can be achieved when

$dP/dV = 0$

$$\frac{d}{dV}\left[V\left[J_0\left(e^{\frac{qv}{KT}} - 1\right) - J_{sc}\right]\right] = 0 \quad (11)$$

Thus the voltage (V_m) at maximum power point is

$$V_m = V_{oc} - \frac{1}{\beta}ln(1 + \square V_m) \quad (12)$$

Where, $\square = \frac{e}{kT}$

The current density (J_m) at maximum power point is

$$J_m = J_0\beta V_m e^{\beta V_m} \cong J_{sc}\left(1 - \frac{1}{\beta V_m}\right) \quad (13)$$

The fill factor (FF) is

$$FF = \frac{V_mJ_m}{V_{oc}J_{sc}} \quad (14)$$

The standard equation of cell efficiency (η) is

$$\eta = \frac{V_{oc}J_{sc}FF}{P_{in}} \times 100\% \quad (15)$$

3. Semiconductor Parameters

The required parameters of different layers of the semiconductor materials, considered in this analysis, are presented in Table 1

Table 1. Semiconductor parameters (at 300K) used in the simulation

Parameter (Unit)	$GaInP_2$ Eg_1 =1.9 eV	GaAs Eg_2 = 1.42 eV	$GaAs_{.96}Bi_{.04}$ Eg_{22}= 1.09 eV	$GaAs_{.95}Bi_{.05}$ Eg_3 =1.0 eV	$GaAs_{.94}Bi_{.06}$ Eg_{33}=0.92 eV	$GaAs_{.92}Bi_{.08}$ Eg_4=0.704 eV
	Top layer for all combination	Second layer for 3J and 4J	Bottom layer for 2J cell	Third layer for 4J cell	Bottom layer for 3J cell	Bottom layer for 4J cell
X (%)		0	4	5	5.83	8.51
λ (m)	0.654×10^{-6}	0.875×10^{-6}	1.138×10^{-6}	1.141×10^{-6}	1.332×10^{-6}	1.775×10^{-6}
M_c	1	1	1	1	1	1
M_v	3	1	1	1	1	1
μ_e (cm^2/Vs)	4000 [17]	2322 [6]	1350 [6]	1350 [6]	1330 [6]	1310 [6]
μ_h (cm^2/Vs)	200 [17]	200 [4]	60 [4]	8 [4]	8 [4]	20 [4]
m_e^*/m_e	0.155 [17]	0.067 [6]	0.067 [6]	0.067 [6]	0.067 [6]	0.067 [6]
m_h^*/m_h	0.460 [17]	0.473 [4]	0.51[4]	0.51[4]	0.51[4]	0.51[4]
$\tau_{SRH\ (S)}$	10^{-5} [17]	10^{-5} [17]	10^{-5} [17]	10^{-5} [17]	10^{-5} [17]	10^{-5} [17]
B ($s^{-1}cm^3$)	7.5×10^{-10} [17]	7.5×10^{-10} [17]	7.5×10^{-10} [17]	7.5×10^{-10} [17]	7.5×10^{-10} [17]	7.5×10^{-10} [17]
N_A (cm^{-3})	10^{17} [17]	9×10^{17}[6]	3.5×10^{17} [6]	3×10^{17}[6]	2×10^{17}[6]	1.5×10^{17}[6]
N_D (cm^{-3})	2×10^{18} [17]	7.8×10^{17}[4]	1.2×10^{17} [4]	5.2×10^{17}[4]	5×10^{17}[4]	2.4×10^{17}[4]
X_n (m)	100×10^{-9}	100×10^{-9}	100×10^{-9}	100×10^{-9}	100×10^{-9}	100×10^{-9}
X_p (m)	208×10^{-9}	300×10^{-9}	300×10^{-9}	400×10^{-9}	400×10^{-9}	500×10^{-9}

4. Result and Discussion

It is worth mentioning that the optoelectronic parameters for the different layers of the semiconductor materials in the stack of cells were considered at 300K and the simulated results are summarized in Table 2 below. The considered input power densities of solar radiation for AM1.5G is $1000W/m^2$ and for AM1.5D is $900W/m^2$ [24, 26]. The simulation has been performed by using our in-house code written for MATLAB (MathWorks Inc.).

Table 2. Simulated results for the effect of the solar spectrum (AM1.5 and AM1.5D) on III-V bismide multijunction solar cells are presented in the following table.

Solar cells	Bandgap (Eg) eV				Airmass (AM)	Bi (x) (%)	J_{sc} (mA/cm^2)	V_{oc} (V)	J_m (mA/cm^2)	V_m (V)	(η) (%)
	Eg_1	Eg_2	Eg_3	Eg_4							
Two junction (2J)	1.09	1.90			AM1.5G	3.93	18.64	2.09	18.40	1.98	36.6
					AM1.5D		17.82	2.09	17.59	1.98	38.7
Three junction (3J)	0.92	1.42	1.90		AM1.5G	5.83	15.65	2.95	15.51	2.84	44.0
					AM1.5D		15.08	2.95	14.94	2.83	47.0
Four Junction (4J)	0.70	1.0	1.42	1.90	AM1.5G	5.00 (Eg_3) & 8.51 (Eg_4)	16.43	3.32	16.30	3.20	52.1
					AM1.5D		16.15	3.32	16.02	3.20	56.4

The energy bandgap of constituent semiconductor materials are judiciously chosen so that the maximum current densities at the maximum power points are the same for all cells that preclude the series connection losses. All the sub-cell are stacked in series for attaining current-matching condition state ensuring the same charge current to flow through the all cells involved. According to Peter Würfel [27], for a given current, the voltages of different layers are determined from the characteristics of the individual cells and then added to give the overall voltage of any multijunction solar cells. The bottom cell with the smaller short-circuit current density determines the total current density. The simulation results presented in Table 2 were estimated by assuming zero losses from reflection, grid coverage, and series resistance. The efficiency values in the far right column of Table 2 are rounded to 1 decimal place. The fill factor FF (not shown in Table 2) were found to be in the range 0.92 – 0.95. Notice that the efficiency of different multijunction solar cells increases up to 2 – 4 % from solar radiation AM1.5G to AM1.5D. This is due to the variation of incident illumination (I) for every individual wavelength (above the bandgap of the material) and total input power density (P_{in}).

The photocurrent depends on the absorption of number of photons and collection efficiency. The stronger intensity solar radiation in the visible range and the deeper penetration of the photons in the infra-red (IR) range enhance the absorption of photons [28]. Therefore, the performance of a solar cell depends on the incident spectrum (i.e., spectral range), the level of irradiance or concentration of the imping radiation and the cell temperature [29]. More specifically, the bandgap of the cell materials, sun concentration, and surface recombination velocity have a significant role in the overall cell efficiency. The impacts of these parameters on the simulated efficiency of different multijunction solar cell are discussed below.

4.1. Effect of Bandgap

In Table 2, it is seen that bandgap of the semiconductor materials is a strong function of solar cell efficiency. Mixing of appropriate mole fraction of bismuth content, Bi(x), with III-V layer allows attaining materials with desired bandgap required for multijunction solar cell. The theoretical cell efficiency is a function of the materials' bandgap [30]. If the top cell bandgap is varied (with Bi content) from 1.70 eV to 1.90 eV [31], efficiency increases linearly from 32.83% to 36.56% for 2J, from 40.89% to 44.04% for 3J and 48.87% to 52.16% for 4J under AM1.5G 1 sun condition. This is presented in Fig. 2(a). We have performed the same studies for a second, third and fourth layer of the cells for both AM1.5G and AM1.5D (As both curves have similar pattern, therefore, curves for AM1.5D are not shown here for clarity).

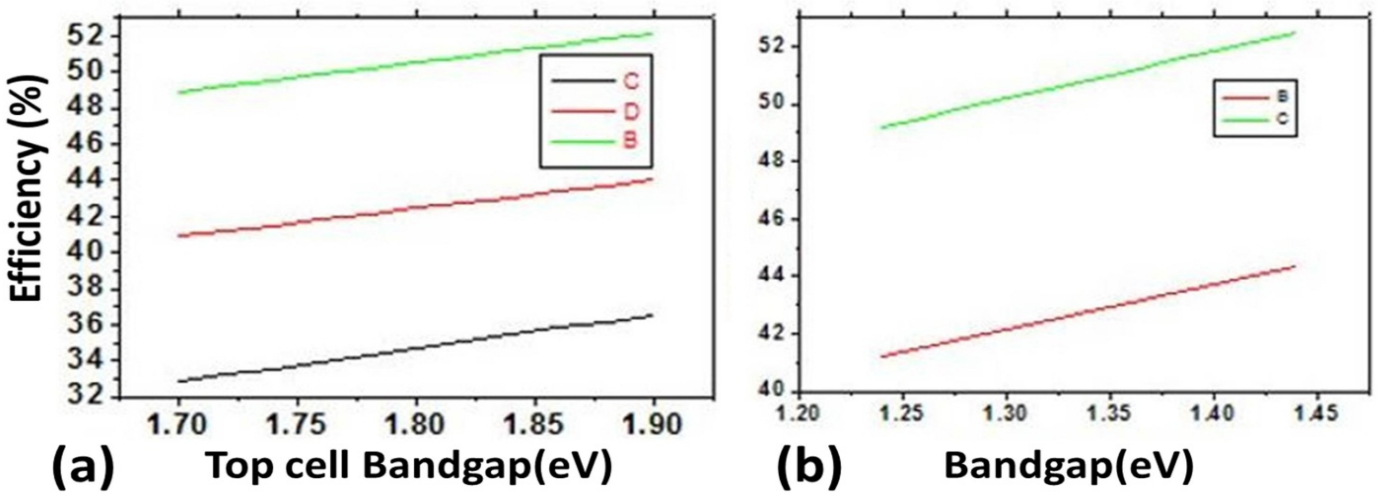

Fig. 2. (a) Bandgap of top cell versus efficiency, where the black curve (C) indicates 2J solar cell, red curve (D) is for 3J solar cell and the green curve is for (B) 4J solar cell; (b) Bandgap of 2nd layer versus efficiency, where the red curve (B) is for 3J solar cell and green curve (C) indicates 4J solar cell.

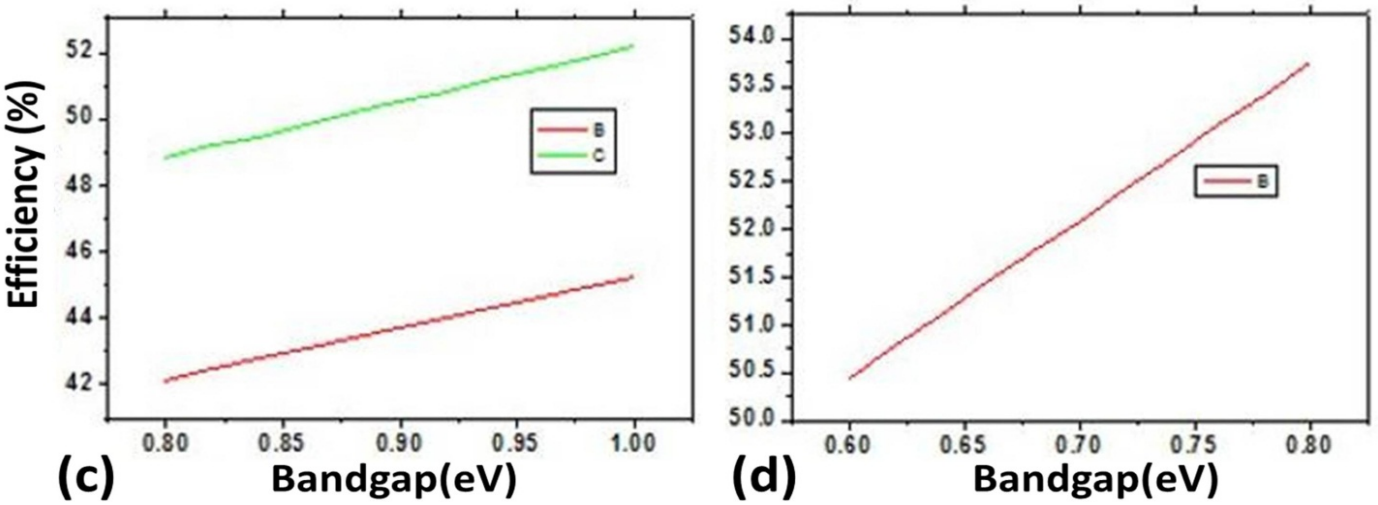

Fig. 2. (c) Bandgap of 3rd layer versus efficiency, where red line (B) is for 3J solar cell and green line (C) is for 4J solar cell; (d) Bandgap of bottom of layer 4J solar cell versus efficiency, where red line (B) indicates its' efficiency.

Again if the bandgap of second layer (bottom layer for 2J solar cell) has been varied from 1.24eV to 1.44eV (for 2J cell 1.09eV to 1.42eV), efficiency is also increased linearly from 36.56% to 42.7% for a 2J, from 41.21% to 44.33% for a 3J and from 49.19% to 52.49% for a 4J under AM1.5G with 1 sun condition which are shown in Fig. 2(b). Again if the bandgap of the third layer (bottom layer of a 3J cell) has been varied from 0.8eV to 1eV, the efficiency also varied from 42.14% to 45.27% for a 3J and 48.87% to 52.16% for a 4J solar cells under AM1.5G with 1 sun condition which are shown in Fig. 2(c). From Fig. 2(d), it is seen that the efficiency is varied from 50.45% to 53.74% by anomalously varying the bandgap from 0.6 eV to 0.8eV with bismuth deposition condition under AM1.5G with 1 sun condition. The above simulation results are suggesting that a ~0.2eV increase in the energy bandgap of bismide layer(s) leads to 3- 4% increase on the overall cell efficiency.

4.2. Effect of Sun concentration

The impacts of sun concentrations have also been analyzed. For that, short circuit current density equation of spectral p-n junction model has been modified by incorporating a concentrator factor (C) with the numerator of the J_{sc} equation (J_{sc}= e $\times\frac{\square I(C)}{hc}$) [9] and with the denominator of the final efficiency equation ($\square = \frac{V_{oc}J_{sc}FF}{(C)P_{in}} \times 100\%$). In this study, sun concentration has been varied from the normal condition, 1 sun, to 500 sun and found that efficiencies of the modeled concentrator multijunction solar cells are increased rapidly

from 1 to 100 sun and then it reaches to a stable value. For AM1.5 G illumination, the efficiencies varied from 36.6 % to 42.5% for a 2J, 44% to 51.6% for a 3J, and 52.1% to 62.5% for a 4J solar cell with the variation of sun concentration from 1 sun to 500 sun shown in Fig. 3(a).

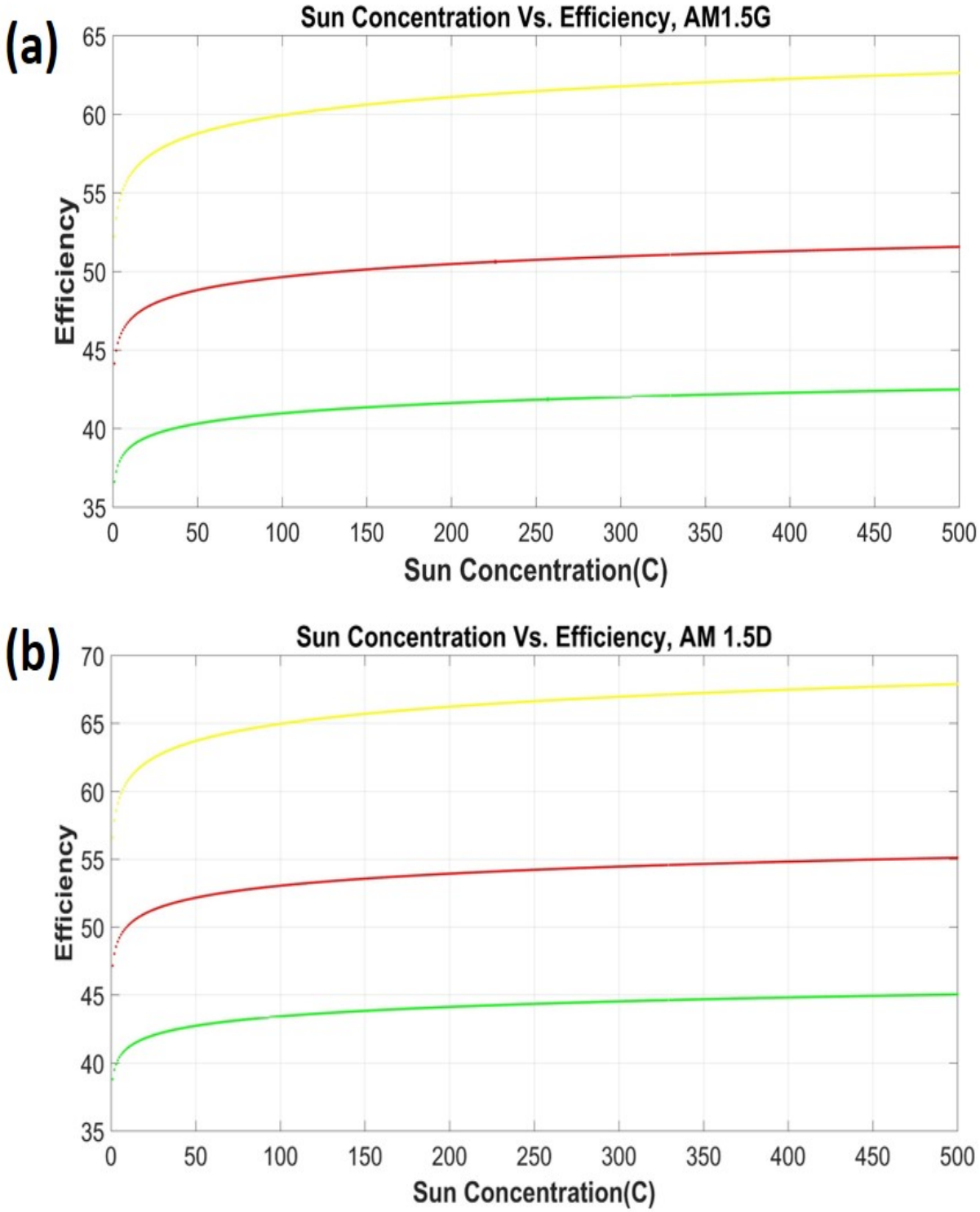

Fig. 3. Sun concentration versus efficiency for (a) AM1.5G and (b) AM1.5D. The top (yellow), middle (red) and bottom (green) curves are, respectively, for 4J, 3J and 2J multijunction solar cells.

Again for AM1.5 D direct normal illumination, the efficiencies varied from 38.7 % to 45% for a 2J, 47% to 55% for a 3J and 56.4% to 67.9% for a 4J solar cell with the variation of sun concentration from 1 sun to 500 sun shown in Fig. 3(b). In fact, the incorporation of concentrator factor with the short-circuit density affects the overall cell performance. When we increase the sun concentration C, the short-circuit current density (J_{sc}= e $\times\frac{\square(C)I}{hv}$), is increased linearly but this linear increment of short-circuit current exponentially increases the open circuit voltage ($V_{oc} = \left(\frac{kT}{e}\right) ln\left[\left(\frac{J_{sc}}{J_0}\right) + 1\right]$), where, symbols stand for the usual meaning. It is observed that the increase of sun concentration will increase the short-circuit current linearly that lead to increase the open circuit voltage exponentially which ultimately lead to increase the overall cell efficiency exponentially (cf. Fig. 3(a) and 3(b)). Moreover, a simple solar cell is nothing but a p-n junction diode under dark. Since open circuit voltage and short-circuit current equations are driven from the diode equation ($J = J_0\left(e^{\frac{qv}{KT}} - 1\right) - J_{ph}$), so the overall solar cell performance-curve will also follow the trend of diode curve. In another words, the diode equation is developed based on the real optoelectronics properties of the semiconductor materials involved, therefore the efficiency also follow the diode like exponential behaviour up to 100 sun and then attains a saturation at higher values of sun concentration, due to practical material limitation (see Fig. 3(a) and 3(b)). The wide variation of simulated efficiency between 1 sun and 500 sun radiation has been appeared in literatures, for example, Marti *et al.* reported the theoretical efficiencies for concentrating solar radiation would be 10-20% higher compared to 1 sun condition [32] and theoretical efficiencies as high as η >60% through different approaches have also been reported by others [26, 33].

4.3. Effect of Surface recombination velocity

From the equations (7) and (8) of present model, it is found that the surface recombination velocity (S_e and S_h) depends on diffusion constant and minority carrier lifetime. Furthermore, the diffusion constant depends on the mobility of the charge carrier; and the minority carrier lifetime depends on donor and acceptor concentrations of the materials involved. To reduce the surface recombination velocity, diffusion constant both for electron and hole must be reduced and the minority carrier lifetime must be increased. Young *et al* [34] reported that the introduction of AlInP layer yielded the lowest surface recombination velocity and the introduction of a buffer with optimized growth temperature yielded the longest minority carrier lifetime. In this work, the surface recombination velocity has been varied from the highest simulated value to zero and the impact of this surface recombination velocity on solar cell performance is presented in Table 3.

Table 3. Simulated results of the surface recombination velocities of different sub-layers and their impact on overall cell efficiencies.

Solar cell	Sub-layer	Simulated surface recombination velocity from our model, S (ms^{-1})		Efficiency for the surface recombination velocity obtained from our model	Zero surface recombination velocity, S (ms^{-1})	Efficiency for zero surface recombination velocity
Two Junction	$GaInP_2$	*Se*1	883.62	36.56% for AM1.5G	0	39.56% for AM1.5G
		*Sh*1	880.81			
	$GaAs_{.96}Bi_{.04}$	*Se*2	957.16	38.75% for AM1.5D		41.93% for AM1.5D
		*Sh*2	118.20			
Three Junction	$GaInP_2$	*Se*1	883.62	44.03%for AM1.5G	0	47.42% for AM1.5G
		*Sh*1	880.81			
	GaAs	*Se*2	2012.6			50.67% for AM1.5D
		*Sh*2	549.87			
	$GaAs_{.94}Bi_{.06}$	*Se*3	710.33	47.04% for AM1.5D		
		*Sh*3	278.61			
Four Junction	$GaInP_2$	*Se*1	883.62	52.13% for AM1.5G	0	56.68% for AM1.5G
		*Sh*1	880.81			
	GaAs	*Se*2	2012.6			
		*Sh*2	549.87			
	$GaAs_{.95}Bi_{.05}$	*Se*3	869.97	56.45% for AM1.5D		61.38% for AM1.5D
		*Sh*3	284.13			
	$GaAs_{.92}Bi_{.08}$	*Se*4	617.52			
		*Sh*4	96.51			

From Table 3, it is clear that if the surface recombination velocity vary from maximum value (according to model) to zero [14], then the efficiency of a 2J solar cell will vary from 36.56% to 39.56% for AM1.5G and 38.75% to 41.93% for AM1.5D under 1 sun condition, the efficiency of a 3J solar cell will vary from 44.03% to 47.42% for AM1.5G and 47.04% to 50.67% for AM1.5D under 1 sun condition and the efficiency of a 4J solar cell will vary from 52.13% to 56.68% for AM1.5G and from 56.45% to 61.38% for AM1.5D under 1 sun condition. Therefore, the efficiency of different multijunction solar cells were found to be increased 3% - 4% when surface recombination velocity reduced to zero from its' maximum simulated value. It can also be seen that the surface recombination velocities of different sub-layers have the exactly equal values for AM1.5G and AM1.5D. In fact, atmospheric conditions such as AM1.5G and AM1.5D do not affect the surface recombination velocities; it depends on semiconductor material properties, such as, diffusion constant, carrier lifetime and mobility of electron and hole.

5. Conclusion

In this study, numerical simulations have been performed to evaluate the performance parameter such as short-circuit current density, open circuit voltage, reverse saturation current density, maximum power, fill factor and efficiencies of a III-V bismide based multijunction solar cells by a modified version of spectral p-n junction model for AM1.5G and AM1.5D under 1 sun condition to 500 sun. The effect of sun concentration, bandgap and surface recombination velocity of the bismide based two-, three-, and four-junction solar cell have been successfully analyzed to realize highly efficient Bismide based multijunction solar cell. Multijunction solar cells are believed to be one of the best alternative means for efficient conversion of sun light to electricity for meeting up future energy demand.

Acknowledgment

This work was financially supported by the Ministry of Science and Technology, the People's Republic of Bangladesh under Special Allocation Project (Grant no.: 39.00.0000.09.06.79.2017/ID-418/422, Date: 06.11.2017).

Declarations of interest: We declare that we have no conflict of interest.

References

[1] G. M. A., H. Yoshihiro, D. E. D., L. D. H., H.-E. Jochen, and H.-B. A. W.Y., "Solar cell efficiency tables (version 52)," Progress in Photovoltaics: Research and Applications, vol. 26, pp. 427-436, 2018.

[2] R. R. King, A. Boca, W. Hong, X. Liu, D. Bhusari, D. Larrabee, et al., "Band-gap-engineered architectures for high-efficiency multijunction concentrator solar cells," in 24th European Photovoltaic Solar Energy Conference and Exhibition, Hamburg, Germany, 2009, p. 55.

[3] S. Wojtczuk, P. Chiu, X. Zhang, D. Derkacs, C. Harris, D. Pulver, et al., "InGaP/GaAs/InGaAs 41% concentrator cells using bi-facial epigrowth," in Photovoltaic Specialists Conference (PVSC), 2010 35th IEEE, 2010, pp. 001259-001264.

[4] D. Beaton, R. Lewis, M. Masnadi-Shirazi, and T. Tiedje, "Temperature dependence of hole mobility in GaAs 1− x Bi x alloys," journal of applied physics, vol. 108, p. 083708, 2010.

[5] D. Cooke, F. Hegmann, E. Young, and T. Tiedje, "Electron mobility in dilute GaAs bismide and nitride alloys measured by time-resolved terahertz spectroscopy," Applied physics letters, vol. 89, p. 122103, 2006.

[6] R. Kini, L. Bhusal, A. Ptak, R. France, and A. Mascarenhas, "Electron hall mobility in GaAsBi," journal of applied physics, vol. 106, p. 043705, 2009.

[7] T. Thomas, A. Mellor, N. Hylton, M. Führer, D. Alonso-Álvarez, A. Braun, et al., "Requirements for a GaAsBi 1 eV sub-cell in a GaAs-based multi-junction solar cell," Semiconductor Science and Technology, vol. 30, p. 094010, 2015.

[8] S. Khanom, M. K. Hossain, F. Ahmed, M. A. Hossain, A. Kowsar, and M. Rahaman, "Simulation study of multijunction solar cell incorporating GaAsBi," in Humanitarian Technology Conference (R10-HTC), 2017 IEEE Region 10, 2017, pp. 432-435.

[9] A. Kowsar and S. F. U. Farhad, "High Efficiency Four Junction III-V Bismide Concentrator Solar Cell: Design, Theory, and Simulation," International Journal of Renewable Energy Research (IJRER), vol. 8, pp. 1762-1769, 2018.

[10] S. Tixier, M. Adamcyk, T. Tiedje, S. Francoeur, A. Mascarenhas, P. Wei, et al., "Molecular beam epitaxy growth of GaAs 1− x Bi x," Applied physics letters, vol. 82, pp. 2245-2247, 2003.

[11] S. Francoeur, M.-J. Seong, A. Mascarenhas, S. Tixier, M. Adamcyk, and T. Tiedje, "Band gap of GaAs 1− x Bi x, 0< x< 3.6%," Applied physics letters, vol. 82, pp. 3874-3876, 2003.

[12] J. Yoshida, T. Kita, O. Wada, and K. Oe, "Temperature dependence of GaAs1-xBix band gap studied by photoreflectance spectroscopy," Japanese journal of applied physics, vol. 42, p. 371, 2003.

[13] A. Kowsar, K. R. Mehzabeen, M. S. Islam, and Z. Mahmood, "Determination of the theoretical efficiency of GaInP/GaAs/GaAs1-xBix multijunction solar cell," in Proc. of the 10th International conf. on fiber optics and Photonics Photonics, India, 2010.

[14] D. Friedman, J. Geisz, A. Norman, M. Wanlass, and S. Kurtz, "0.7-eV GaInAs junction for a GaInP/GaAs/GaInAs (1eV)/GaInAs (0.7 eV) four-junction solar cell," in 2006 IEEE 4th World Conference on Photovoltaic Energy Conversion, 2006.

[15] S. M. Sze and K. K. Ng, Physics of semiconductor devices: John wiley & sons, 2006.

[16] M. E. Nell and A. M. Barnett, "The spectral pn junction model for tandem solar-cell design," IEEE Transactions on Electron Devices, vol. 34, pp. 257-266, 1987.

[17] S. R. Kurtz, P. Faine, and J. Olson, "Modeling of two□ junction, series□connected tandem solar cells using top□ cell thickness as an adjustable parameter," Journal of Applied Physics, vol. 68, pp. 1890-1895, 1990.

[18] M. A. H. Abu Kowsar, Md Sofikul Islam, Afrina Sharmin and Z. H. Mahmood, "Analysis of theoretical efficiencies of GaInP2/GaAs/Ge multijunction solar cell," The Dhaka University Journal of Applied Science and Engineering, vol. 3, 2015.

[19] A. Kowsar, A. Y. Imam, M. Rahaman, M. S. Bashar, M. S. Islam, S. Islam, et al., "Comparative study on the efficiencies of silicon solar cell."

[20] S. N. Sakib, S. P. Mouri, Z. Ferdous, A. Kowsar, and M. S. Kaiser, "Effect of different solar radiation on the efficiency of GaInP2/GaAs/Ge based multijunction solar cell," in Electrical Information and Communication Technology (EICT), 2015 2nd International Conference on, 2015, pp. 528-532.

[21] M. I. A Kowsar, KR Mehzabeen, ZH Mahmood, "Study on the Efficiency of the GaInP2/GaAs/Ge Multijunction Solar Cell," in Proc. of International Conference on Environmental Aspects of Bangladesh,BEN, Japan, 2010, pp. 116-119.

[22] S. N. Sakib, S. P. Mouri, A. Kowsar, M. Rahaman, and M. S. Kaiser, "Theoretical efficiency of AlAs/GaAs/GaAs0. 91Bi0. 085 based new multijunction solar cell and effects of solar radiation and sun concentration on it," in Microelectronics, Computing and Communications (MicroCom), 2016 International Conference on, 2016, pp. 1-6.

[23] A. Dilan, "Quantum photovoltaic effect: Two photon process in solar cell," in Renewable Energy Research and Applications (ICRERA), 2015 International Conference on, 2015, pp. 1084-1088.

[24] D. R. Myers, K. Emery, and C. Gueymard, "Revising and validating spectral irradiance reference standards for photovoltaic performance evaluation," Journal of solar energy engineering, vol. 126, pp. 567-574, 2004.

[25] A. Standard, "G173,“Standard Tables for Reference Solar Spectral Irradiances: Direct Normal and Hemispherical on 37 Tilted Surface,” Amer," Society for Testing Matls., West Conshocken PA, USA, 2007.

[26] S. Kurtz, D. Myers, W. McMahon, J. Geisz, and M. Steiner, "A comparison of theoretical efficiencies of multi□ junction concentrator solar cells," Progress in Photovoltaics: research and applications, vol. 16, pp. 537-546, 2008.

[27] P. WÃ, Physics of Solar cells: from Principles to new Concepts: John Wiley & Sons, 2008.

[28] S.-W. Feng, C.-M. Lai, C.-H. Chen, W.-C. Sun, and L.-W. Tu, "Theoretical simulations of the effects of the indium content, thickness, and defect density of the i-layer on the performance of p-i-n InGaN single homojunction solar cells," Journal of applied physics, vol. 108, p. 093118, 2010.

[29] S. Kurtz and J. Geisz, "Multijunction solar cells for conversion of concentrated sunlight to electricity," Optics express, vol. 18, pp. A73-A78, 2010.

[30] R. King, D. Law, C. Fetzer, R. Sherif, K. Edmondson, S. Kurtz, et al., "Pathways to 40%-efficient concentrator photovoltaics," in Proc. 20th European Photovoltaic Solar Energy Conference, 2005, pp. 10-11.

[31] S. Kurtz, J. Olson, and A. Kibbler, "Electroreflectance and photoreflectance of GaInP," Solar Cells, vol. 24, pp. 307-312, 1988.

[32] A. Marti and G. L. Araújo, "Limiting efficiencies for photovoltaic energy conversion in multigap systems," Solar Energy Materials and Solar Cells, vol. 43, pp. 203-222, 1996.

[33] M. A. Green, Third generation photovoltaics: Springer, 2006.

[34] M.-J. Yang, M. Yamaguchi, T. Takamoto, E. Ikeda, H. Kurita, and M. Ohmori, "Photoluminescence analysis of InGaP top cells for high-efficiency multi-junction solar cells," Solar Energy Materials and Solar Cells, vol. 45, pp. 331-339, 1997.